Engineering Journal issn: 0125-8281

Article

Mechanical and Thermal Neutron Attenuation Properties of Concrete Reinforced with Low-Dose Gamma Irradiated PETE Fibers and Sodium Borate

Sarayut Khemngern[1,a], Doonyapong Wongsawaeng[1,b], Pitcha Jongvivatsakul[2,c,*], and Peem Nuaklong[2,d]

1 Department of Nuclear Engineering, Faculty of Engineering, Chulalongkorn University, Bangkok, 10330, Thailand
2 Innovative Construction Materials Research Unit, Department of Civil Engineering, Faculty of Engineering, Chulalongkorn University, Bangkok, 10330, Thailand

Email: [a]sarayutk@outlook.co.th, [b]doonyapong.w@chula.ac.th, [c]pitcha.j@chula.ac.th (Corresponding author), [d]peenua@gmail.com

Abstract. This research investigated the mechanical and thermal neutron attenuation properties of concrete reinforced with low-dose gamma irradiated polyethylene terephthalate (PETE) fibers. Low dose (20 – 60 kGy) gamma irradiated PETE fibers of 1.3 and 25 denier size were uniformly mixed with concrete at 0.1%, 0.2%, and 0.3% volume fraction. The results showed that the fiber reinforced concrete (FRC) having 25 denier fibers provided higher compressive strength, flexural strength, and toughness than FRC with 1.3 denier fibers. Moreover, addition of PETE fibers in the concrete enhanced thermal neutron attenuation; however, both fibers exhibited no significant difference in thermal neutron attenuation ability. In addition, this study investigated the effects of adding sodium borate, a boron-containing compound, in concrete mixed with PETE at various proportions. It was found that when sodium borate powder was added, the compressive strength of the concrete decreased, whereas the thermal neutron attenuation ability significantly increased with respect to sodium borate content.

Keywords: Gamma ray, polyethylene-terephthalate, fibers, mechanical properties, thermal neutron attenuation, sodium borate.

ENGINEERING JOURNAL Volume 24 Issue 3
Received 7 July 2019
Accepted 18 February 2020
Published 31 May 2020
Online at http://www.engj.org/
DOI:10.4186/ej.2020.24.3.1

1. Introduction

Concrete is a widely used material nowadays, primarily in civil engineering works such as buildings, bridges, roads, and as a neutron shielding material in locations where neutron radiation is presented. Neutron particles produced by nuclear reactions are extremely harmful to living organisms because they can interact with hydrogen atoms that are the major component of living tissues. This will lead to free radical formations in the tissues and bloodstream as well as many negative effects that will follow from the body interacting with neutrons.

Up to date, many researchers have innovated neutron shielding materials. Polyethylene terephthalate (PETE) fibers were applied as a reinforcing agent to enrichment concrete strength as well as to shield against slow neutrons. Khemngern et al. [1] intensified the indissolubility of PETE fibers in a concentrated basic solution characteristic of concrete (pH = 12) using low-dose gamma radiation to convince crosslinking of the polymeric chains. Results demonstrated that gamma ray dose of only 30 kGy responded in the excellent molecular weight, tensile strength and degree of crystallinity of PETE fibers. The surface topology using SEM micrography were also appraised. An accelerated age testing exposed that these radiation-treated fibers will stabilize their mechanical strength in concrete for up to at least 60 months. Slow neutron attenuation test of fiber-reinforced concrete (FRC) showed that the degree of slow neutron shielding increased with the addition of PETE fiber. Therefore, these FRCs can be utilized as an effective neutron shielding material for nuclear and radiation applications to enhance radiation safety. However, the mechanical properties of PETE fiber reinforced concrete have not been reported.

So far, the effect of boron carbide on radiation attenuation of cement composited has been studied. Grossman et al. [2], Abdo et al. [3], and Abdullah et al. [4] present composite concrete materials for neutron shielding by mixing boron carbide powder in concrete. Results revealed that the neutron shielding efficiency was higher with increasing amount of boron carbide powder, but the compressive strength decreased. Nyarku et al. [5] and Sarıyer et al. [6] mixed boron carbide and ferro-boron in concrete to fabricate a neutron shielding material. It was found that boron was an excellent low-energy neutron absorber, and iron acted to effectively reduce the energy of fast neutrons to become thermal neutrons before they were absorbed by boron. Thus, concrete mixed with boron and iron can be a very effective fast neutron shielding material [5, 6]. Kharita et al. [7, 8] studied incorporation of boron-containing materials into concrete as a radiation shielding material. Results indicated that mixing boric acid into concrete resulted in cement hardening problems. However, the use of up to 1% of boron compounds did not affect the mechanical properties of concrete materials. In addition, the fabrication of composite materials made from boron and carbon fibers produced in the form of sandwich have been introduced as a material for neutron shielding [9-13]. It was concluded that as the boron content increased, the neutron shielding capability of the material increased. An appropriate production process could also improve the material's thermal stability [9, 11]. Therefore, boron is found to be effective for neutron shielding. Based on the literature, there is no study mixing sodium borate, which is one of boron compound, in concrete for neutron shielding.

The present research introduced the composite concrete materials which can attenuate low-energy neutrons by incorporating polyethylene terephthalate (PET or PETE) fibers and sodium borate. Sodium borate was selected because it composes of inexpensive elemental boron, which exhibits high microscopic cross-section for neutron capturing, resulting in high neutron capturing capability. The mechanical properties and the ability to attenuate low-energy neutrons of PETE fiber reinforced concrete with and without sodium borate have been investigated. As no researcher has studied the low-energy neutron attenuation efficiency of composite concrete materials reinforced with PETE fibers and sodium borate as well as the mechanical properties, this study will provide new information for the scientific community that could be applied for practical uses.

2. Materials and Methods

2.1. Materials

2.1.1. PETE fibers

The preparation process of PETE fibers presented by Khemngern et al. [1] is adopted in this study. The PETE fibers were gamma irradiated at 40 kGy using Gamma 220 Excel gamma cell with a cobalt-60 source at Thailand Institute of Nuclear Technology (public organization) with an absorbed dose rate of approximately 5 kGy/h and an irradiator temperature of approximately 40°C. The properties of fibers are shown in Tables 1 and 2. Figures 1 and 2 display the SEM micrographs of the irradiated PETE fibers at low gamma ray dose at 200X and 5,000X magnification, respectively. It can be observed from the SEM micrographs that the fibers did not degrade physically with low-dose gamma ray as the surface appeared smooth.

Table 1. Un-irradiated PETE fiber properties [1].

Property	Value
Density [1]	1.37 g/cm^3
Glass transition temperature (T_g) [2]	67 ˚C
Melting temperature [3]	254.3 ˚C
Degree of crystallinity [3]	39.68
Number average molecular weight (MW) [4]	22455 ± 196 g/mol

[1] Measurement operated at 25 ˚C; [2] Operated using differential scanning calorimeter (DSC, Netzsch, DSC204F1) with temperature increasing rate of 10 ˚C/min and temperature range of -100 to 300 ˚C; [3] Operated using XRD (Bruker, D8 Advance); [4] Measured using membrane osmometry method.

Table 2. Irradiated PETE fiber properties.

Name	Size (Denier; D)	Diameter (mm)	Length (mm)	Density at 25 ˚C (g/cm^3)	Melting temperature (°C)
1.3D	1.3	0.014	32	1.37	254.3
25D	25	0.059			

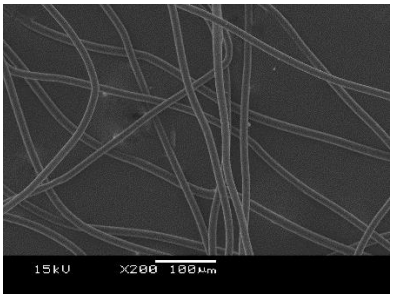

Fig. 1. SEM micrograph of fibers (200X, 15 kV).

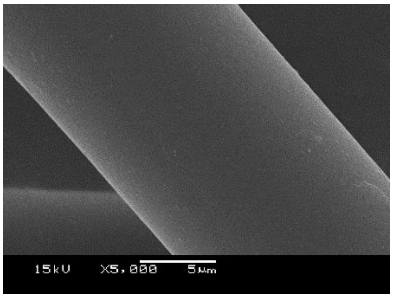

Fig. 2. SEM micrograph of fibers (5,000X, 15 kV).

Table 3. Mix proportions of concrete.

Series	Name	Cement (kg/m^3)	Water (kg/m^3)	Fine aggregate (kg/m^3)	Coarse aggregate (kg/m^3)	Admixture (kg/m^3)	Fiber type	Fiber content (%)	Sodium borate (%)
I	OPC	465	200	697	999	2.33	-	0.0	0.0
	1.3D-0.1	465	200	697	999	4.65	1.3D	0.1	
	1.3D-0.2						1.3D	0.2	
	1.3D-0.3						1.3D	0.3	
	25D-0.1	465	200	697	999	4.65	25D	0.1	
	25D-0.2						25D	0.2	
	25D-0.3						25D	0.3	
II	25D-0.0-B0.1	465	200	697	999	4.65	25D	0.0	0.1
	25D-0.1-B0.1						25D	0.1	
	25D-0.2-B0.1						25D	0.2	
	25D-0.3-B0.1						25D	0.3	
	25D-0.0-B0.2	465	200	697	999	4.65	25D	0.0	0.2
	25D-0.1-B0.2						25D	0.1	
	25D-0.2-B0.2						25D	0.2	
	25D-0.3-B0.2						25D	0.3	
	25D-0.0-B0.4	465	200	697	999	4.65	25D	0.0	0.4
	25D-0.1-B0.4						25D	0.1	
	25D-0.2-B0.4						25D	0.2	
	25D-0.3-B0.4						25D	0.3	

2.1.2. Concrete

Table 3 summarized the mix proportion of concrete. The water-to-cement ratio was constant at 0.43 for all mixes. Ordinary Portland cement (Type 1), water, fine aggregate, coarse aggregate, and polycarboxylic ether-based superplasticizers (PCEs) admixture were used in mixtures. The compositions of Portland cement comprise four mainly chemical oxides: 57.7% CaO, 23.6% SiO_2, 5.3% Al_2O_3 and 3.5% Fe_2O_3. The well-graded natural river sand with specific gravity of 2.64, dry-rodded unit weight of 1,664 kg/m^3 and fineness modulus of 2.84 was used as fine aggregate. The coarse aggregate used in this study was crushed limestone with maximum aggregate size of 19 mm. The weight of admixture was 0.5% by cement weight for concrete without fibers and 1.0% by cement weight for fiber reinforced concrete. As seen in Table 3, specimens are divided into 2 series. Series I consist of concrete specimens without sodium borate. The effect of sodium borate is investigated from the specimens in Series II. In this study, two sizes of irradiated PETE fibers, which were 1.3 denier (1.3D) and 25 denier (25D), were used. For both fiber sizes, the fiber volume was 0.1%, 0.2%, and 0.3% of concrete volume as presented in Table 3. Sodium borate used in the experiments was deca-hydrated of $Na_2B_4O_7$ with 0%, 0.1%, 0.2%, and 0.4% by cement weight. In Table 3, OPC denotes plain concrete without fiber. 1.3D-*x* denotes concrete with *x*% of 1.3 denier fibers and 25D-*x*-B*y* denotes concrete with *x*% of 25 denier fibers and *y*% of sodium borate.

2.2. Concrete Casting

The concrete was mixed using a pan mixer. For fiber reinforced concrete, concrete was firstly mixed, after that PETE fibers were dispersedly mixed into the fresh concrete. For the specimens in Series II, sodium borate was dry mixed with cement first, followed by ~~the~~ other ingredients. Then, fibers were added into flesh concrete. The specimens were demolded after 24 hour and cured in water for 28 days. The concrete specimens were removed from water and left for one day before performing the compressive test, flexural test, and neutron attenuation test.

2.3. Specimens and Test Methods

2.3.1. Properties of flesh and hardened concrete

In order to measure the property of fresh concrete, slump tests were operated in accordance with ASTM C143 [14] using a mould with an upper diameter of 100 mm, a lower diameter of 200 mm and height of 300 mm. Additionally, the mechanical properties of hardened concrete which are compressive strength, flexural strength, and toughness were determined. The compressive test was operated in accordance with ASTM C39 [15] for cylindrical specimens with 150 mm diameter and 300 mm height. The flexural test was operated according to ASTM C1609 [16] using concrete beams with dimensions 100 × 100 × 350 mm^3. The prismatic specimens were tested on a 300 mm span. Figure 3 presents a concrete specimen subjected to a bending test. In order to obtain a load–deflection curve, a load cell was installed to measure the applied load and two transducers were used to measure deflections during the test. Results from the load–deflection curves were used for calculating the flexural strength from Eq. (1) and toughness, which is defined as the area under the load–deflection curve from deflection of 0 to $L/150$ (= 2 mm.) [16].

$$f = \frac{PL}{bd^2} \tag{1}$$

where f is flexural strength; P is maximum load; L is span length; b is width of specimen; and d is depth of specimen.

Fig. 3. Flexural performance test of fiber reinforced concrete.

2.3.2. Thermal neutron attenuation test

The testing method for thermal neutron attenuation in this study is referred from Khemngern et al. [1]. Concrete specimens for the neutron attenuation test were in a cubical shape with the dimension on each side of 100 mm. In order to perform the test, a concrete sample was placed on a platform as illustrated in Fig. 4. High energy neutrons from a neutron source underwent thermalization by elastic collision with paraffin materials to become low energy neutrons before passing the concrete specimen. 241-Americium-Berylium with the dose rate of 29.08 mR/h was used as the neutron source. A BF_3 proportional tube was used to detect thermal neutrons passing through the specimen. Neutron attenuation can be calculated from Eq. (2).

$$NAT(\%) = \frac{I - P}{I} \times 100 \tag{2}$$

where NAT is thermal neutrons attenuation percentage; I is the number of thermal neutrons impinging on specimen; and P is the number of thermal neutrons passing through specimen.

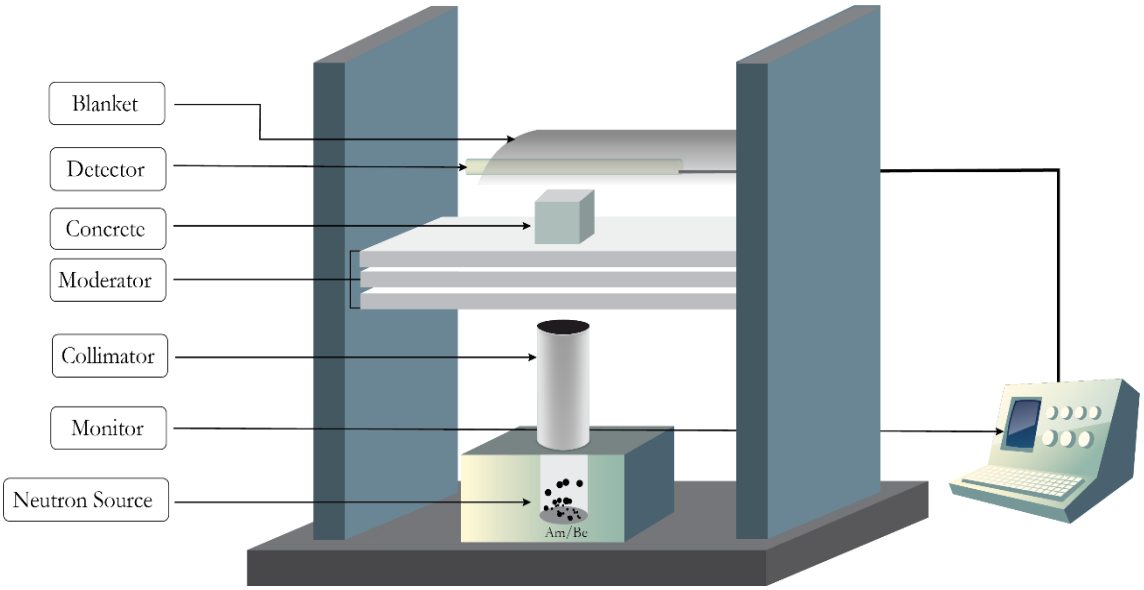

Fig. 4. Thermal neutron attenuation test setup [1].

3. Results and Discussions

3.1. Properties of PETE Fiber Reinforced Concrete

3.1.1. Concrete slump

Slump of the specimens in Series I is shown in Table 4. Results indicate that the slump decreased with the increase in fiber volume fraction. This occurs due to the fact that the inclusion of fibers increased the internal friction within the concrete, especially when the high content of fibers is used [17]. The concrete containing 0.3% 1.3D fibers showed the lowest workability, with 74% decrease in slump value than control concrete. However, the role of 25D fibers with respect to concrete workability is not clear. The slump of concrete slightly increases with of 25D fibers up to 0.1%, then decreases with the fibers.

3.1.2. Compressive strength

The average compressive strengths from 3 replicated specimens are shown in Fig. 5. The results show that the compressive strengths slightly increase with the addition of PETE fibers. However, the addition of PETE fiber beyond 0.2% reduced the compressive strength. This is because the higher fiber content of PETE led the balling effect of fibers (agglomeration of fibers) as also observed in fiber reinforced concrete with other fiber types [18, 19], thus creating the weak zones in concrete. It should be noted that the smaller the fiber size (smaller diameter or shorter length), the higher the chances of fiber agglomeration [18]. This may explain why the compressive strengths of concrete reinforced with 25D fibers are greater than those of 1.3D fibers as seen from Fig. 5.

3.1.3. Flexural strength and toughness

Figure 6 illustrates the load-deflection curves of the flexural tests. The curves exhibit a linear characteristic up to the peak load, after which the load decreases with the increase in deflection. The softening behaviour of PETE fiber reinforced concrete can be captured as shown in Fig. 6. It is observed that, in the post-peak behaviour of specimens with PETE fibers, the specimens can resist higher load compared to that of OPC at the same deflection. The values of average flexural strength calculated from 3 specimens are plotted in Fig. 7. The results indicate that incorporating 1.3D and 25D fibers at 0.1% - 0.3% fiber content significantly increased the flexural strength of concrete compared to that of OPC. The clear tendency of the effect of fiber content on flexural strength could not be observed. This may be due to the small fiber size and low volume fraction used in this study. However, the flexural strength decreased when 0.3% of 25D were added because of the low concrete slump which results in the increase of voids inside concrete.

Values of toughness at deflection of $L/150$ according to ASTM C1609 [16] are shown in Fig. 8. Although both fiber sizes can increase toughness compared to that of OPC, reinforcement of 1.3D fibers gives slightly lower toughness than 25D in 0.2% and 0.3% fiber contents. In addition, toughness of specimens with 1.3D are almost constant in spite of the fact that the fiber content of 1.3D increases. The most likely explanation is that the fiber size was very small (14 μm) and, thus, it did not increase the toughness when the volume fraction increased. On the other hand, toughness of specimen containing 25D fibers increase when 0.3% of fibers are used.

DOI:10.4186/ej.2020.24.3.1

Table 4. Experimental results of specimens in Series I.

Mixes	Fiber type	Fiber Content (%)	Slump (cm)	Compressive Strength (MPa)	Flexural Strength (MPa)	Toughness (N-m)	Thermal neutrons attenuation* (%)
OPC	-	0.0	14.5	49.8	3.61	7.86	35.48
1.3D-0.1	1.3D	0.1	11.3	52.3	4.83	13.49	44.05
1.3D-0.2	1.3D	0.2	9.0	57.2	4.63	12.65	49.90
1.3D-0.3	1.3D	0.3	3.7	49.3	4.88	12.61	56.24
25D-0.1	25D	0.1	18.0	57.1	4.94	13.57	44.00
25D-0.2	25D	0.2	8.5	62.7	4.95	13.39	50.10
25D-0.3	25D	0.3	4.8	58.1	4.14	14.81	57.90

*Khemngern et al. [1].

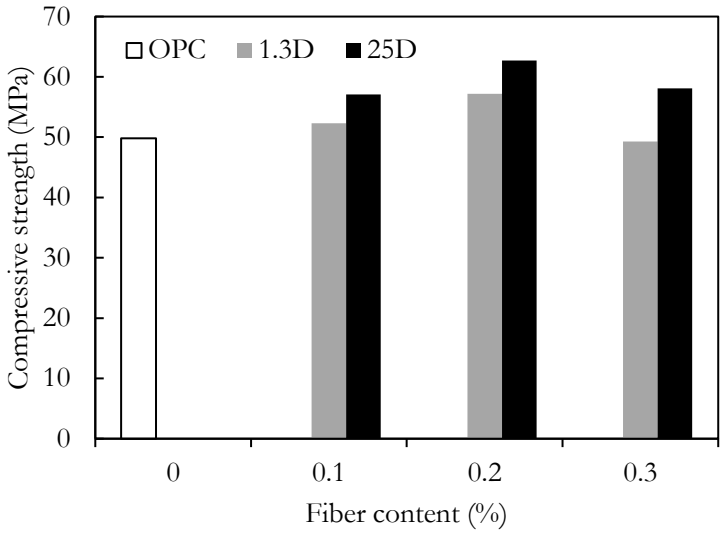

Fig. 5. Compressive strength of concrete in Series I.

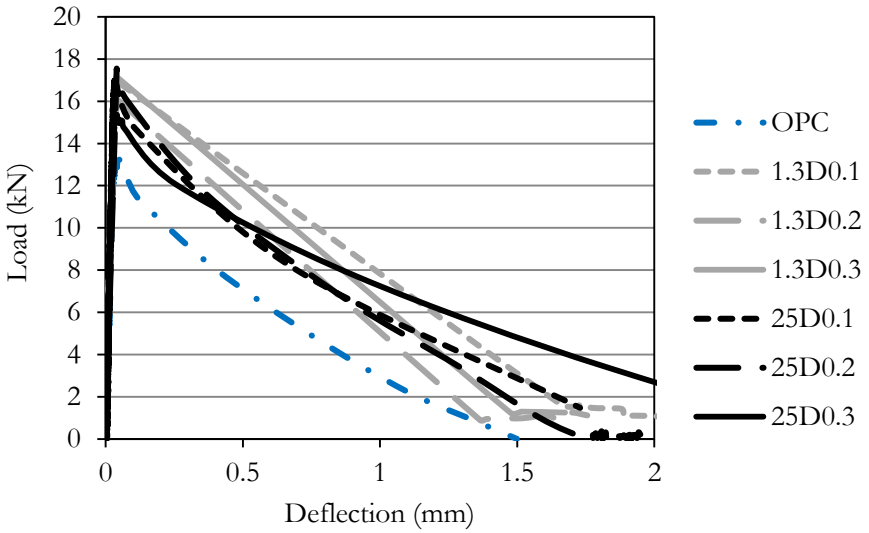

Fig. 6. Load-deflection curves of plain concrete and PETE fiber reinforced concrete.

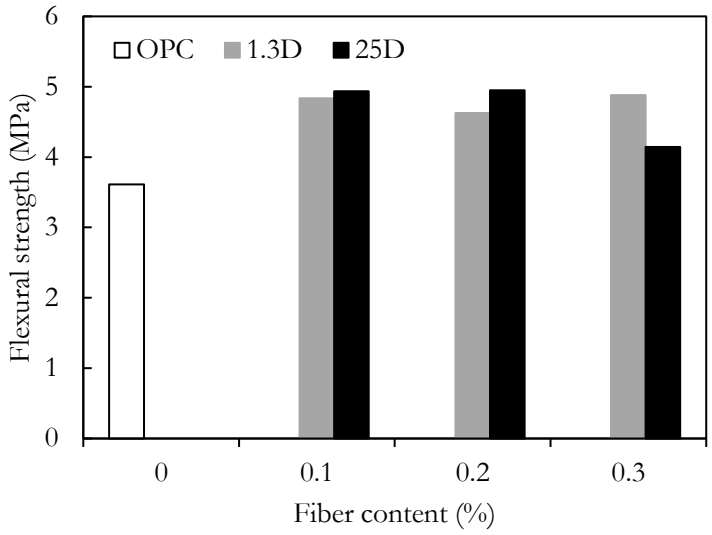

Fig. 7. Flexural strength of plain concrete and PETE fiber reinforced concrete

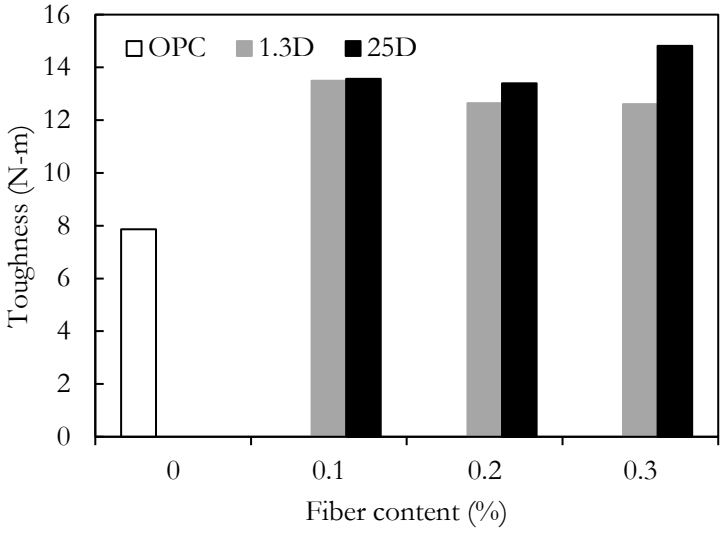

Fig. 8. Toughness at deflection of L/150

3.1.4. Proposed mixture for fiber reinforced neutron shielding concrete

As shown in Table 1, the addition of radiation-treated PETE fibers significantly improves thermal neutron attenuation of concrete compare to that of OPC. This is because the hydrogen content in PETE fibers, which are composed of long hydrocarbon chains, is higher than that in OPC. As hydrogen is a very effective fast neutron moderator and thermal neutron absorber, by incorporating a material with higher hydrogen content, thermal neutron attenuation will be enhanced. In addition, it was observed that the degree of thermal neutron attenuation was slightly affected by the fiber size as a large fiber size resulted in marginally better thermal neutron shielding. This is most likely because large fibers exhibit more physical cross-sectional areas than smaller ones, so thermal neutron interaction was slightly enhanced [20].

In conclusion, PETE fibers which were properly dosed with gamma radiation can be applied in reinforced concrete materials to be used as an effective neutron shield for radiation protection. However, when considering both mechanical properties and thermal neutron attenuation, it is suggested that 25D fibers are more suitable for using as fiber reinforced neutron shielding concrete since they provided higher compressive strength, flexural strength, toughness than 1.3D fibers. The 0.2-0.3% of 25D-PETE fibers are the optimal values of mix design for neutron shielding concrete.

3.2. Properties of PETE Fiber Reinforced Concrete with Sodium Borate

According to the results presented in previous chapter, 25D fibers were selected to further investigate the effect of PETE fibers and sodium borate on the compressive strength of concrete and thermal neutron attenuation. Mix

proportions of concrete specimens in this chapter (Series II) are summarized in Table 3. The PETE fiber volume fractions were 0%, 0.1%, 0.2%, and 0.3%, and sodium borate was added at 0%, 0.1%, 0.2%, and 0.4% by cement weight. The results of specimens in Series II are discussed as follows:

3.2.1. Compressive strength

The compressive strength of PETE fiber reinforced concrete with sodium borate is demonstrated in Fig. 9. It was found that when adding sodium borate to the concrete, the compressive strength was reduced in all fiber contents. For example, the compressive strength of concrete mixture containing 0.1% 25D fibers decreased approximately 9%, 37% and 55% when 0.1%, 0.2% and 0.4% of sodium borate were added, respectively. During the Portland cement hydration, sodium borate normally acts as retarder by: (1) preventing the growth of calcium silicate hydrate (CSH) [21]; and (2) inhibiting the crystallization of calcium hydroxide [22]. These mechanisms are responsible for low strength development.

3.2.2. Thermal neutron attenuation

The results of thermal neutron attenuation of concrete reinforced with PETE fibers and sodium borate are presented in Fig. 10. It is clear that the thermal neutron attenuation of the concrete increases with the addition of PETE fibers as well as the addition of sodium borate. Since the microscopic cross-section for thermal neutron absorption of boron (B-10) is 759 barns, whereas that of hydrogen (H-1) is 0.332 barn, the boron component (with natural enrichment) of sodium borate acts as a very effective thermal neutron absorber. From Fig. 10, plain concrete without PETE fiber and sodium borate can attenuate thermal neutrons by approximately 35.48%, whereas the thermal neutron attenuation of concrete with 0.3% of fibers (without sodium borate) is approximately 57.9%. When sodium borate is added to the concrete, the thermal neutron attenuation increased substantially. By adding 0.4% sodium borate and 0.3% of 25D fibers, thermal neutrons can be attenuated up to 82.16%. This result agrees with the expectation because the microscopic thermal neutron absorption cross-section of B-10 is much higher than that of H-1. Thus, it can be concluded that the addition of PETE fibers and sodium borate substantially improves thermal neutron attenuation efficiency of concrete.

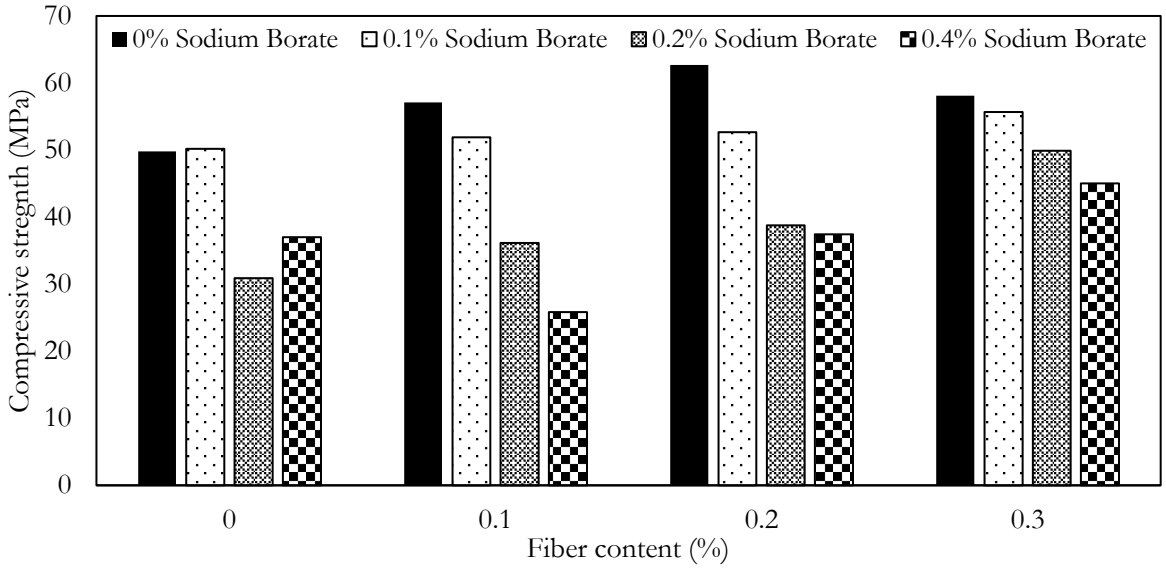

Fig. 9. Compressive strength of PETE fiber reinforced concrete with and without sodium borate.

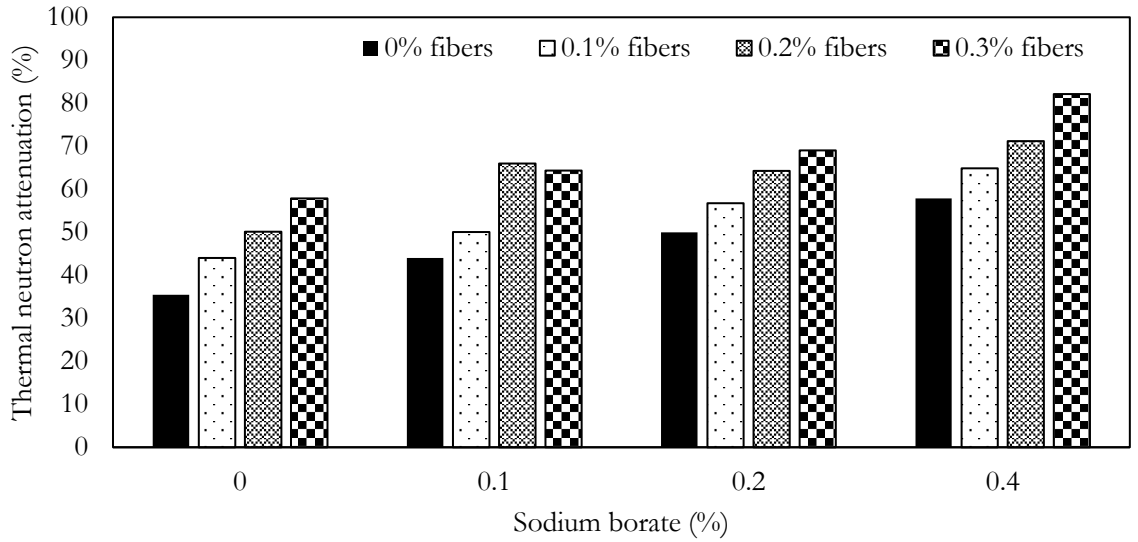

Fig. 10. Thermal neutron attenuation of concrete reinforced with PETE fibers and sodium borate.

4. Conclusion

Based on the study of the properties of concrete reinforced with PETE fibers irradiated with low-dose gamma ray, the following conclusions can be established.

1. The mechanical properties of concretes improved with the addition of PETE fibers, especially for the flexural strength and toughness. In general, reinforcement of 25D fibers resulted in a higher compressive strength, flexural strength, and toughness than 1.3D fibers.
2. According to the results of mechanical properties and thermal neutron attenuation, the optimal volume fractions of PETE fibers for developing the neutron shielding fiber reinforce concrete are 0.2% and 0.3% since they give the compromising results between mechanical properties and thermal neutron radiation shields.
3. Increasing sodium borate content resulted in decreasing compressive strength of the concretes; however, reinforcement with both sodium borate and PETE resulted in better thermal neutron attenuation, which was significantly higher than reinforcement with only PETE. Thus, the produced concrete materials can be utilized to absorb low-energy neutrons, although the materials should not bear substantial loads as the addition of sodium borate powder reduced the compressive strength.

Acknowledgments

This research has been supported by the scholarship from the Graduated School, Chulalongkorn University to commemorate The Celebrations on the Auspicious Occasion of Her Royal Highness Princess Maha Chakri Sirindhorn's 5th cycle (60th) Birthday and The 90th Anniversary Chulalongkorn University Fund (Ratchadaphiseksomphot Endowment fund). Authors are pleased to credit the help of Ang-Tai Company, Department of Nuclear Engineering, Chulalongkorn University.

References

[1] S. Khemngern, D. Wongsawaeng, P. Jongvivatsakul, D. Swantomo, and K. T. Basuki, "Enhancement of stability in alkali solution of polyethylene terephthalate fibers using low-dose gamma irradiation for fiber-reinforced neutron shielding concrete," *Engineering Journal*, vol. 23, no. 2, pp. 11-21, 2019.

[2] A. A. Grossman, R. P. Doerner, S. Luckhardt, R. Seraydarian, and A. K. Burnham, "Transport properties of hydrogen isotopes in boron carbide structures," *Journal of Nuclear Materials*, vol. 266, pp. 819-824, 1999.

[3] A. E. S. Abdo, M. A. M. Ali, and M. R. Ismail, "Influence of magnetite and boron carbide on radiation attenuation of cement–fiber/composite," *Annals of Nuclear Energy*, vol. 30, no. 4, pp. 391-403., 2003.

[4] Y. Abdullah, M. R. Yusof, A. Muhamad, Z. Samsu, and N. E. Abdullah, "Cement-boron carbide concrete as radiation shielding material," *Journal of Nuclear and Related Technologies*, vol. 7, no. 2, pp. 74-79, 2010.

[5] M. Nyarku, R. S. Keshavamurthy, V. D. Subramanian, A. Haridas and E. T. Glover, "Experimental neutron attenuation measurements in possible fast reactor shield materials," *Annals of Nuclear Energy*, vol. 53, pp. 135-139, 2013.

[6] D. Sarıyer, R. Küçer, and N. Küçer, "Neutron shielding properties of concretes containing boron carbide and ferro–boron," *Procedia-Social and Behavioral Sciences*, vol. 195, pp. 1752-1756, 2015.

[7] M. H. Kharita, M. Takeyeddin, M. Alnassar, and S. Yousef, "Development of special radiation shielding concretes using natural local materials and evaluation

of their shielding characteristics," *Progress in Nuclear Energy*, vol. 50, no. 1, pp. 33-36, 2008.

[8] M. H. Kharita, S. Yousef, and M. Al Nassar, "Review on the addition of boron compounds to radiation shielding concrete," *Progress in Nuclear Energy*, vol. 53, no. 2, pp. 207-211, 2011.

[9] S. E. Gwaily, M. M. Badawy, H. H. Hassan, and M. Madani, "Natural rubber composites as thermal neutron radiation shields: I. B4C/NR composites," *Polymer Testing*, vol. 21, no. 2, pp. 129-133, 2002.

[10] Y. Huang, L. Liang, J. Xu, and W. Zhang, "The design study of a new nuclear protection material," *Nuclear Engineering and Design*, vol. 248, pp. 22-27, 2012.

[11] Y. Huang, W. Zhang, L. Liang, J. Xu, and Z. Chen, "A "Sandwich" type of neutron shielding composite filled with boron carbide reinforced by carbon fiber," *Chemical Engineering Journal*, vol. 220, pp. 143-150, 2013.

[12] J. J. Park, S. M. Hong, M. K. Lee, C. K. Rhee, and W. H. Rhee, "Enhancement in the microstructure and neutron shielding efficiency of sandwich type of 6061Al–B_4C composite material via hot isostatic pressing," *Nuclear Engineering and Design*, vol. 282, pp. 1-7, 2015.

[13] P. Wang, X. Tang, H. Chai, D. Chen and Y. Qiu, "Design, fabrication, and properties of a continuous carbon-fiber reinforced Sm_2O_3/polyimide gamma ray/neutron shielding material," *Fusion Engineering and Design*, vol. 101, pp. 218-225, 2015.

[14] *Standard Test Method for Slump of Hydraulic-Cement Concrete*, American Society for Testing and Materials, ASTM C143, West Conshohocken, PA, 2015.

[15] *Standard Test Method for Compressive Strength of Cylindrical Concrete Specimens*," American Society for Testing and Materials, ASTM C39, West Conshohocken, PA, 2018.

[16] *Standard Test Method for Flexural Performance of Fiber-Reinforced Concrete (Using Beam With Third-Point Loading)*, American Society for Testing and Materials, ASTM C1609, West Conshohocken, PA, 2019.

[17] A. H. Alani, N. M. Bunnori, A. T. Noaman and T. A. Majid, "Durability performance of a novel ultra-high-performance PET green concrete (UHPPGC)," *Construction and Building Materials*, vol. 209, pp. 395-405, 2019.

[18] A. Le Hoang and E. Fehling, "Influence of steel fiber content and aspect ratio on the uniaxial tensile and compressive behavior of ultra high performance concrete," *Construction and Building Materials*, vol. 153, pp. 790-806, 2017.

[19] S. Grünewald and J. C. Walraven, "Parameter-study on the influence of steel fibers and coarse aggregate content on the fresh properties of self-compacting concrete," *Cement and Concrete Research*, vol. 31, no. 12, pp. 1793-1798, 2001.

[20] G. Odian, *Principle of Polymerization*, 4 ed. New York: Wiley-Interscience, 2003.

[21] B. Li, X. Ling, X. Liu, Q. Li, and W. Chen, "Hydration of Portland cements in solutions containing high concentration of borate ions: Effects of LiOH," *Cement and Concrete Composites*, vol. 102, pp. 94-104, 2019.

[22] L. Zhang, Y. Ji, J. Li, F. Gao, and G. Huang, "Effect of retarders on the early hydration and mechanical properties of reactivated cementitious material," *Construction and Building Materials*, vol. 212, pp. 192-201, 2019.

Sarayut Khemngern, photograph and biography not available at the time of publication.

Doonyapong Wongsawaeng, photograph and biography not available at the time of publication.

Pitcha Jongvivatsakul, photograph and biography not available at the time of publication.

Peem Nuaklong, photograph and biography not available at the time of publication.